# Synthesis, characterization, and properties of novel novolac epoxy resin containing naphthalene moiety

Guoyuan Pan [a], Zhongjie Du [a], Chen Zhang [a], Congju Li [b], Xiaoping Yang [a], Hangquan Li [a,*]

[a] *The Key Laboratory of Beijing City on Preparation and Processing of Novel Polymer Materials,*
*Beijing University of Chemical Technology, Beijing 100029, PR China*
[b] *Beijing Key Laboratory of Clothing Material R&D and Assessment, Beijing Institute of Clothing Technology, Beijing 100029, PR China*

## Abstract

A series of novel novolac epoxy resins containing naphthalene moiety with different molecular weights were synthesized via condensation of bisphenol A and 1-naphthaldehyde, followed by epoxidation with epichlorohydrin. The chemical structure of the naphthalene epoxy thus obtained was characterized using FTIR, ^{1}H NMR spectra and GPC analyses. The naphthalene epoxy was cured with 4,4′-diaminodiphenyl sulfone (DDS) and the cured products were characterized with thermogravimetric analysis, dynamic mechanical analysis, and X-ray diffraction. Compared with the diglycidyl ether of bisphenol A (DGEBA), the cured naphthalene epoxy resin showed remarkably higher glass transition temperatures ($T_g$s), enhanced thermal stability and better moisture resistance. When the molar ratio of 1-naphthaldehyde to bisphenol A was 0.67, the optimal thermal resistance was observed.
© 2007 Elsevier Ltd. All rights reserved.

*Keywords:* Epoxy resin; 1-Naphthaldehyde; Bisphenol A

## 1. Introduction

Epoxy resins have good thermal and dimensional stability, excellent chemical and corrosion resistance, and superior mechanical and electrical properties, in addition to ease of handling and processabilities, therefore found wide applications in aerospace and electronic industries as surface coatings, structural adhesives, printed circuit board, insulation materials for electronic devices, and advanced composites matrices. In high-tech applications, however, epoxy resins with lower thermal expansion, higher toughness, better heat and moisture resistance were required. For this reason, modifications of epoxy resins, in both backbone and pendant groups have been continuously attempted in order to improve their thermal and physical properties [1−3].

Many studies have been reported for improving the heat resistance of epoxy resins by increasing the crosslinking density of cured epoxy resin [4] or introducing bulky structures such as biphenyl or naphthalene [5,6]. The introduction of naphthalene moiety is expected to greatly improve the thermal property and moisture resistance [7,8]. Xu et al. have synthesized novel epoxy resin bearing naphthyl and limonene moieties which showed remarkably higher $T_g$, lower coefficient of thermal expansion, higher thermal stability, better moisture resistance, and dielectric property [9]. Kaji and Endo have reported that the cured polymer obtained from epoxy resin containing naphthalene structure showed higher $T_g$, higher flexural modulus, lower thermal expansion, and lower moisture absorption [10]. Tsung-Han Ho reported that a naphthalene containing aralkyl epoxy resin made from the difunctional naphthol showed a low coefficient of thermal expansion, high heat resistance, and low moisture absorption [11]. The thermal stability or $T_g$ of naphthalene-based epoxy resins was higher than that of phenyl-based epoxy resins [12]. However, there have been no reports on modifying diglycidyl ether of bisphenol A (DGEBA) by introducing naphthalene moiety to improve thermal resistance and physical properties.

\* Corresponding author. Tel./fax: +86 10 64428804.
*E-mail address:* duzj@mail.buct.edu.cn (H. Li).

In this paper, a series of novolac epoxy resins containing naphthalene moiety with different molecular weights were synthesized via adjusting the ratios of naphthalene/bisphenol A ranging from 0.5 to 2.0. Firstly, the monomer of 1-naphthaldehyde was introduced into the backbone of bisphenol A, followed by epoxidation with epichlorohydrin, the epoxy resins containing naphthalene moiety were obtained. The thermal resistance and mechanical properties of the cured system were investigated and compared with those neatly based on bisphenol A. The naphthalene epoxies showed higher thermal and physical properties.

## 2. Experimental

### 2.1. Materials

Bisphenol A (BPA) was obtained from Tianjin Jinke Fine Chemical Co., China. 1-Naphthaldehyde was purchased from Jiangsu Mingfeng Chemical Co., China. Diglycidyl ether of bisphenol A (DGEBA, epoxy equivalent weight, EEW 196) was obtained from Wuxi Resin Factory, China with commercial code of E51. $p$-Toluene sulfonic acid (PTSA) (supplied by Guangdong Xilong Chemical Co., China) was used as a catalyst. Epichlorohydrin (ECH), isopropanol and methyl isobutyl ketone (MIBK), were supplied by Beijing Chemical Co., China, and were distilled before use. 4,4′-Diaminodiphenyl sulfone (DDS) used as curing agent was obtained from Shanghai Chemical Co., China.

### 2.2. Synthesis of bisphenol A−naphthaldehyde novolac resin (bis-NANR) [13−15]

A 200 ml methyl isobutyl ketone (MIBK) solution containing 68.4 g bisphenol A (BPA, 0.3 mol) and 1.43 g $p$-toluene sulfonic acid (PTSA, 0.0075 mol) was added to 500 ml four-neck round-bottom flask, equipped with a heating mantle, mechanical stirrer, thermocouple, temperature controller, and a Dean−Stark trap with a reflux condenser. After purging with nitrogen for 10 min, the solution was heated to 100 °C with stirring. 1-Naphthaldehyde (5.3 g) was introduced dropwise to the solution for about 1 h. Subsequently, the temperature of the flask was kept at 120 °C for 5 h allowing the reaction

to occur. Water generated during the reaction was removed via azeotropic distillation with MIBK.

After the reaction completion, the above solution was washed with deionized water until the solution became neutral. The organic phase was finally evaporated at 180 °C under vacuum to remove the unreacted 1-naphthaldehyde and solvent. The remaining solid product was washed five times with a mixture of water/methanol (68:32 v/v) to remove the unreacted BPA. A red-brown solid product was obtained after vacuum-drying.

In this work, 1-naphthaldehyde and BPA were used at various molar ratios. When the mole ratios of 1-naphthaldehyde to BPA were 0.50, 0.67, 0.80, 1.00, 1.25, 1.50, 1.75, and 2.00, the corresponding resins obtained were denoted as $N_{0.50}$, $N_{0.67}$, $N_{0.80}$, $N_{1.00}$, $N_{1.25}$, $N_{1.50}$, $N_{1.75}$, and $N_{2.00}$. The synthetic scheme is shown in Fig. 1.

### 2.3. Synthesis of bisphenol A−naphthaldehyde novolac epoxy resin (bis-NANER) [13−15]

One of above synthesized novolac resins containing naphthalene (2.4 g), epichlorohydrin (277.19 g), and isopropanol (64 ml) were added to 500 ml four-neck round-bottom flask. After thoroughly mixed at room temperature, the mixture was heated to 70 °C for 5 min. Subsequently, 32 g aqueous sodium hydroxide solution with 20 wt% concentration was introduced dropwise to the bis-NANR solution with stirring. The system was maintained at 70 °C for additional 4 h, and the bottom brine layer was removed by siphoning. The remaining product was further reacted with 16 g aqueous NaOH with 20 wt% concentration at 70 °C for 1 h. Finally, the product in the flask was washed five times with deionized water to remove the residual sodium chloride, and the excess epichlorohydrin was evaporated under vacuum to give a light brown-colored solid product. In this work, when the resins $N_{0.50}$, $N_{0.67}$, $N_{0.80}$ and $N_{1.00}$ were used, the corresponding naphthalene epoxies obtained would be denoted as $NE_{0.50}$, $NE_{0.67}$, $NE_{0.80}$, and $NE_{1.00}$. The general scheme of this preparation is shown in Fig. 2.

### 2.4. Curing of epoxy resins

An epoxy resin was heated to 120 °C under vacuum to remove air bubbles and moisture. Subsequently the epoxy resin
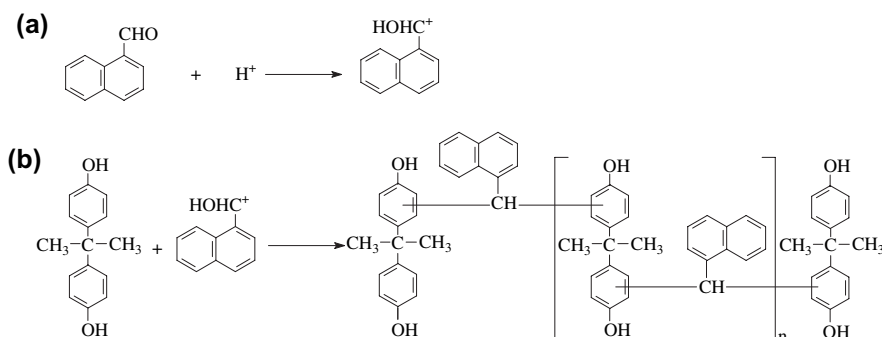


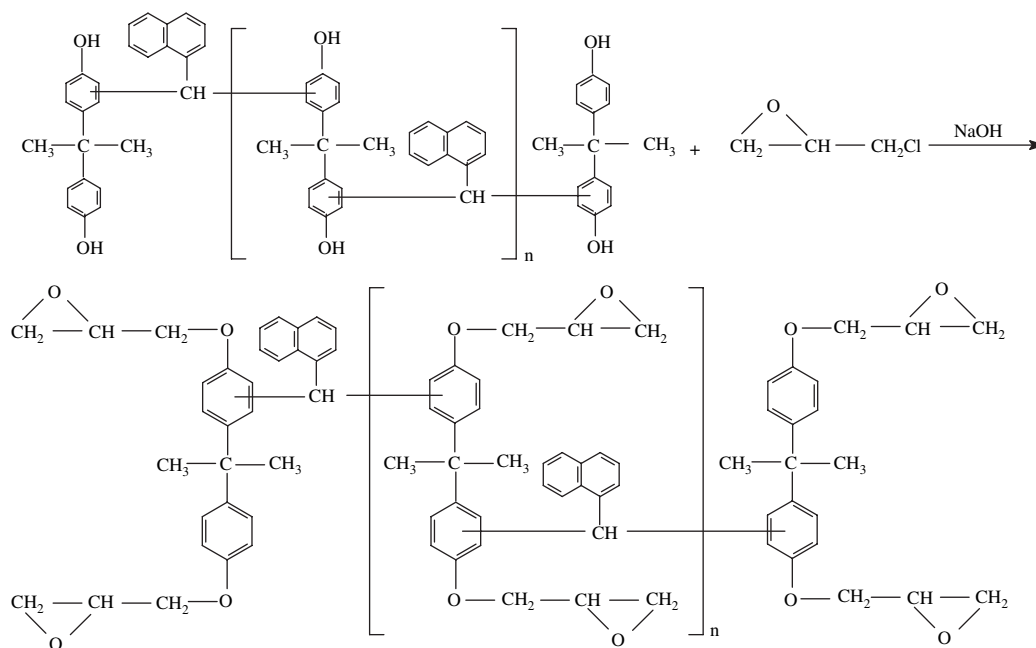Fig. 1. Schematic diagram of the synthesis of bis-NANR.

Fig. 2. Schematic diagram of the synthesis of bis-NANER.

was heated to 150 °C to mix with a stoichiometric amount of curing agent (DDS). The mixture was cured at 160 °C for 2 h, followed by curing at 200 °C for 10 h, and finally postcured at 220 °C for 4 h.

## 2.5. Characterization

FTIR spectra were recorded on a Nexus 670 infrared spectrometer. Gel permeation chromatography (GPC) was performed using a PE series 200 GPC instrument equipped with Styragel columns (HT3_HT5_HT6E). Tetrahydrofuran (THF) was used as eluent at 30 °C at a flow rate of 1.0 ml/min. $^1$H nuclear magnetic resonance ($^1$H NMR) characterization were carried out by Bruker AV-600 NMR spectrometer using acetone-$d_6$ as the solvent and tetramethylsilane (TMS) as internal standard.

The epoxy equivalent weights (EEWs) of epoxy resin were determined by HCl/acetone titration method. Gel content measurements were performed in a Soxhlet extractor using acetone as solvent under refluxing at 100 °C for 24 h. Dynamic viscoelastic properties were measured using a Rheometric Scientific DMTA-V instrument using 2 mm × 5 mm × 30 mm rectangular samples at a programmed heating rate of 5 °C/min from 50 °C to 300 °C at a frequency of 1 Hz under nitrogen atmosphere.

Thermogravimetric analysis (TGA) was performed by a NETZSCH STA 449C TG-DSC simultaneous analyzer at a heating rate of 10 °C/min under nitrogen atmosphere. Wide-angle X-ray diffraction patterns (WAXD) were obtained using a Rigaku D/max-2400 diffractometer at room temperature using copper filtered Cu Kα radiation (40 kV, 200 mA).

Moisture absorption was determined as follows: the samples (⌀ 50 mm × 1 mm) were dried under vacuum at 100 °C

for 12 h, and then cooled to room temperature. The samples were weighed and placed in 100 °C water for 72 h and weighed again. The moisture absorption was calculated as percent weight gain: Moisture absorbance $\% = (W/W_o - 1) \times 100\%$, where $W$ is the weight of the sample after dipping in 100 °C water for 72 h, $W_o$ is the weight of the sample after placing in vacuum oven for 12 h.

## 3. Results and discussion

### 3.1. FTIR and $^1$H NMR spectra characterizations

Fig. 3 shows the FTIR spectra of 1-naphthaldehyde (trace a), bisphenol A (trace b), bisphenol A–naphthaldehyde novolac resin (bis-NANR) (trace c), and naphthyl epoxy resin (bis-NANER) (trace d). The assignments of traces c and d are shown in Table 1. The reaction between 1-naphthaldehyde and
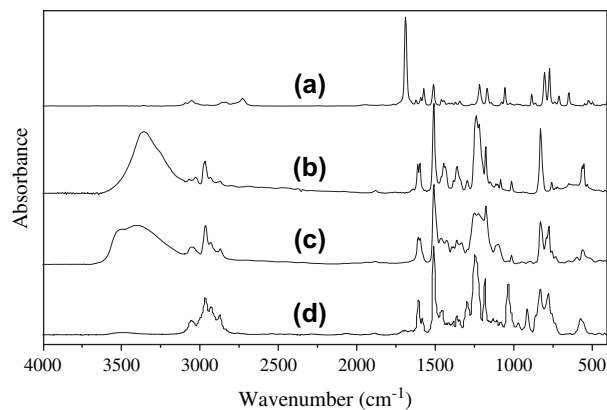


Fig. 3. FTIR spectra of (a) 1-naphthaldehyde; (b) bisphenol A; (c) bis-NANR; and (d) bis-NANER.

Table 1
Wavenumbers (cm$^{-1}$) and assignment of IR bands of bis-NANR and bis-NANER

| Bis-NANR | Approximate assignment | Bis-NANER | Approximate assignment |
|---|---|---|---|
| 3406 | $\nu$O–H | 3450 | $\nu$O–H |
| 3051 | $\nu$C–H (aromatic ring) | 3054 | $\nu$C–H (aromatic ring) |
| 2964 | $\nu_{as}CH_3$ | 2965 | $\nu_{as}CH_3$ |
| 2930 | $\nu CH_2$ | 2928 | $\nu CH_2$ |
| 2869 | $\nu_s CH_3$ | 2871 | $\nu_s CH_3$ |
| 1608 | $\nu$C=C (aromatic ring) | 1607 | $\nu$C=C (aromatic ring) |
| 1597 | | 1582 | |
| 1509 | | 1510 | |
| 1463 | $\delta CH_2 + \delta_{as}CH_3$ | 1457 | $\delta CH_2 + \delta_{as}CH_3$ |
| 1384 | $\delta_s CH_3$ | 1385 | $\delta_s CH_3$ |
| 1363 | $\delta$OH (phenolic) + $\delta$CH | 1362 | $\delta$CH |
| 1250 | $\tau CH_2 + \delta CH_2$ | 1246 | $\nu$R + $\tau CH_2 + \delta CH_2$ |
| 1225 | $\nu$C–O (phenol) | 1184 | $\nu$C–C(Ph–C(C)–Ph) |
| 1178 | $\nu$C–C (Ph–C(C)–Ph) | 1108 | $\nu$(C–O–C) |
| | | 1035 | aliphatic ether |
| | | 971 | $\gamma$CH(Ph) |
| | | 914 | $\delta$Oxirane ring |
| 829 | $\gamma$CH 1,4 and/or 1,2,4-substituted Ph | 830 | $\gamma$CH 1,4 and/or 1,2,4-substituted Ph |
| 796 | $\gamma$CH ($\alpha$-nap.) | 796 | $\gamma$CH ($\alpha$-nap.) |
| 776 | | 780 | |

Ph, phenyl ring; R, epoxy ring; $\nu$, stretching vibration; a, antisymmetric; s, symmetric; $\delta$, in plane deformation; $\tau$, twisting vibrations; $\gamma$, out-of-plane deformation.

BPA was confirmed by the disappearance of the C=O stretching absorption peak at 1689 cm$^{-1}$, and the appearance of characteristic absorption peak of $\alpha$-naphthalene out-of-plane deformation at 776 cm$^{-1}$ (trace c). The disappearance of peak at around 3406 cm$^{-1}$ (trace c) with the appearance of characteristic peak at 914 cm$^{-1}$ (trace d) suggested the completion of etherification of naphtholic hydroxyl.

Fig. 4(a)–(c) shows the $^1$H NMR spectra of bis-NANR (N$_{0.67}$), bis-NANER (N$_{0.67}$), and BPA, respectively. For bis-NANR, multiplet at 1.202–1.411 ppm, 1.556–1.633 ppm, 6.627–7.067 ppm, 7.391–7.865 ppm, and 8.024–8.186 ppm (Fig. 4(a)) can be attributed to methane bridges (–CH–C$_{10}$H$_7$), methyl, aromatic (–C$_6$H$_5$), aromatic (–C$_{10}$H$_7$), and hydroxyl protons, respectively. Methine (–CH–C$_{10}$H$_7$) bridge was the characteristic structure of bis-NANR, which can be obviously noticed by comparing with the $^1$H NMR spectrum of BPA in Fig. 4(c). In addition, two multiplets corresponding to the aromatic protons on the phenol ring at 6.692–6.728 ppm (*ortho* to the phenolic hydroxyl group) and 7.016–7.058 ppm (*meta* to the phenolic hydroxyl group) were observed symmetrical about a central point, this was because that BPA is a *para*-substituted aromatic compound in which two substitutes differ from each other in electronic effects. However, compared with the $^1$H NMR spectrum of BPA, the symmetrical patterns of bis-NANR became complex and some split peaks appear between 6.728–7.016 ppm, which was assigned to the effect of the methine (–CH–C$_{10}$H$_7$) bridges bonding to the BPA phenyl rings.

In fact, the eight reactive sites on BPA for the methine (–CH–C$_{10}$H$_7$) bridges to bond to the BPA phenyl rings can be categorized into two kinds, *ortho* and *meta* positions [16–18]. The two kinds of positions appeared to possess the same bonding chance to the methine (–CH–C$_{10}$H$_7$) bridges, which was indicated by the ratio of the peak areas for the two kinds of aromatic protons. Moreover, the ratios of area integrations for peak (Ph–CH(–C$_{10}$H$_7$)–Ph/aromatic protons/Ph–C–CH$_3$) (Fig. 4(a)) were consistent with the proposed statistical structures of bis-NANR shown in Fig. 1.

In the $^1$H NMR spectrum of bis-NANER (Fig. 4(b)), the same signal pattern as in bis-NANR was observed, except for the signals corresponding to the glycidyl group. The chemical shifts are assigned as follows: 1.202–1.411 ppm (multiplet, methane bridges (–CH–C$_{10}$H$_7$) protons), 1.629 ppm (singlet, methyl protons), 2.693–2.849 ppm (multiplet, protons of methylene in the oxirane ring), around 3.292 ppm (multiplet, protons of methine in the oxirane ring), 3.835–4.298 ppm (multiplet, protons of methylene connected the phenoxy and the oxirane ring), 6.729–6.870 ppm, 6.936–7.165 ppm (multiplet, aromatic protons on phenoxy ring), and 7.411–7.880 ppm (multiplet, protons of naphthalene moiety). These results can support the structure of bis-NANER, shown in Fig. 2.

### 3.2. GPC measurements

Fig. 5(a) and (b) presents the GPC traces for samples (N$_{0.67}$) prepared by direct refluxing and azeotropic distillation, respectively. The calculated molecular weight and polydispersity index (PDI) were listed in Table 2. It was clear that the $\overline{M}_n$ based on azeotropic distillation method was almost twice that of direct refluxing method. Because the condensation of formaldehyde phenol resin was reversible, increase in concentration of reagents or decrease in concentration of products was favorable to the reaction. In the direct refluxing method, the water in the system promoted the inverse reaction, consequently lower molecular weight of the product was resulted. Whereas in the azeotropic distillation method, water was removed by Dean–Stark trap from the system and thus facilitated the condensation, higher $\overline{M}_n$ of bis-NANR was obtained. For this reason, the azeotropic distillation method was exclusively utilized in this work.

The average molecular weights ($\overline{M}_n$ and $\overline{M}_w$) and PDI through GPC measurements are shown in Table 3. One can see that the molecular weights increased with increasing the fraction of 1-naphthaldehyde. This may be due to the excess 1-naphthaldehyde that led to large branched structures. Since BPA had eight reactive sites it may act as a curing agent when 1-naphthaldehyde was in excess [16–18]. When the concentration of 1-naphthaldehyde was larger than BPA, large branched structures were generated. Such branched structures resulted not only larger molecular weights, but also wider molecular weight distributions. Further increasing the fraction of 1-naphthaldehyde, the gel point would be reached and local network structures occurred. The gel contents in bis-NANR are shown in Table 4. It showed that the gel occurrence started from the mole ratio of 1-naphthaldehyde to BPA of 1.25. The
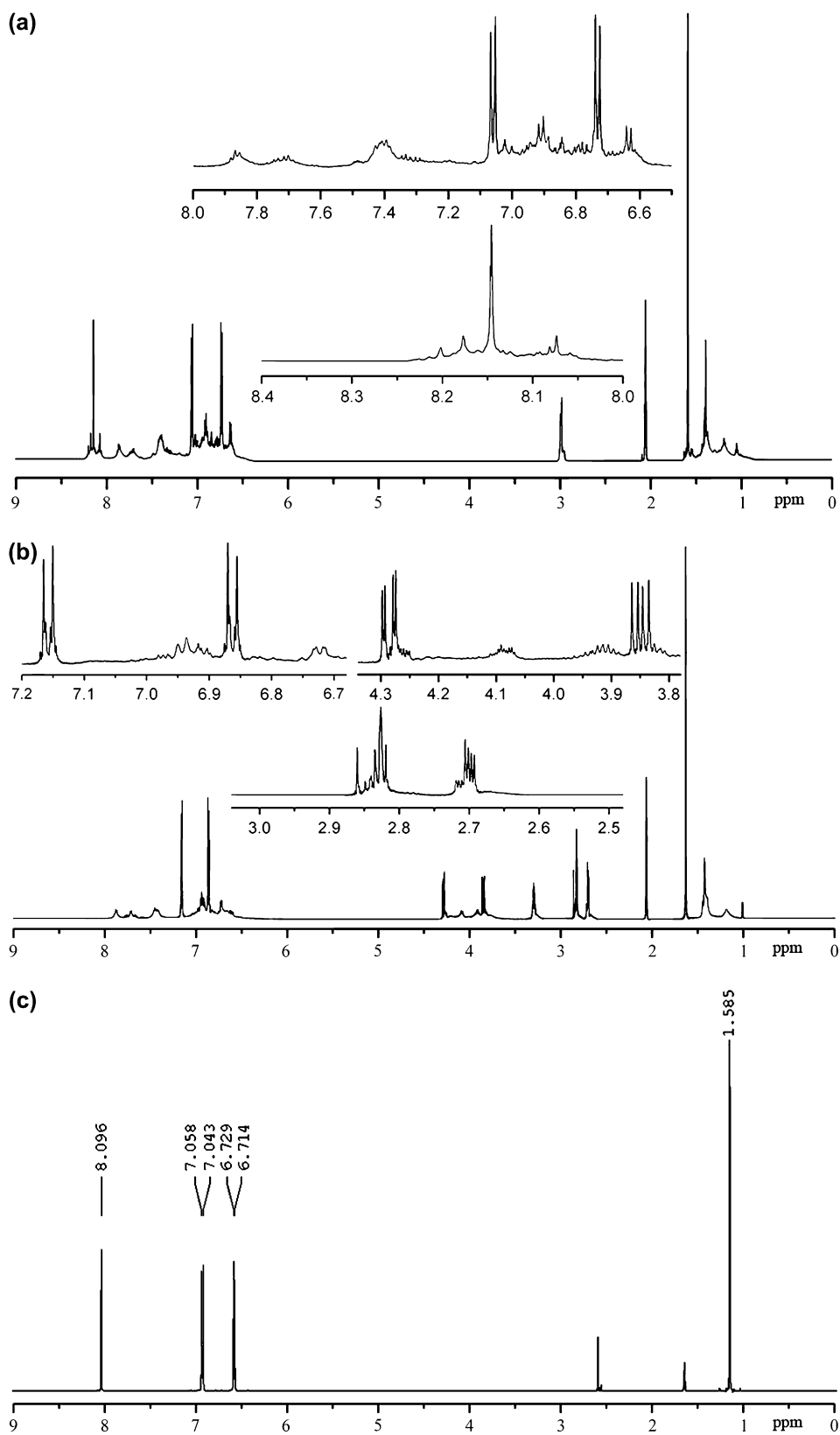
**(a)**



**(b)**



**(c)**



Fig. 4. $^1$H NMR spectra of (a) bis-NANR; (b) bis-NANER; and (c) bisphenol A.
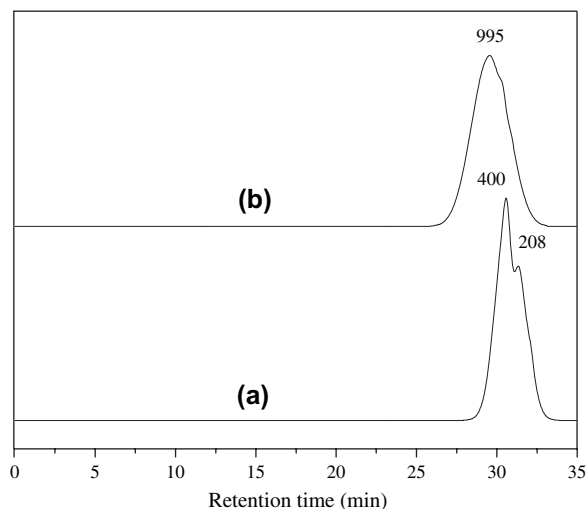
Fig. 5. Gel permeation chromatogram of sample (a) direct refluxing and (b) azeotropic distillation.

Table 2
Average molecular weights and molecular polydispersity index (PDI) of bis-NANR

| Method | $\overline{M}_n$ | $\overline{M}_w$ | PDI $(\overline{M}_w/\overline{M}_n)$ |
|---|---|---|---|
| Direct refluxing | 348 | 462 | 1.33 |
| Azeotropic distillation | 813 | 1571 | 1.93 |

Table 3
Average molecular weights and molecular polydispersity index of bis-NANR

| Sample code | Ratio of 1-naphthaldehyde/BPA | $\overline{M}_n$ | $\overline{M}_w$ | PDI $(\overline{M}_w/\overline{M}_n)$ |
|---|---|---|---|---|
| N$_{0.50}$ | 0.50:1 | 608 | 1036 | 1.70 |
| N$_{0.67}$ | 0.67:1 | 813 | 1571 | 1.93 |
| N$_{0.80}$ | 0.80:1 | 1244 | 2613 | 2.10 |
| N$_{1.00}$ | 1.00:1 | 1377 | 3683 | 2.67 |
| N$_{1.25}$ | 1.25:1 | – | – | – |

Table 4
The effect of ratio of 1-naphthaldehyde/BPA on the gel content of bis-NANR

| Sample code | Ratio of 1-naphthaldehyde/BPA | Gel content (%) |
|---|---|---|
| N$_{1.00}$ | 1.00:1 | 0.00 |
| N$_{1.25}$ | 1.25:1 | 19.09 |
| N$_{1.50}$ | 1.50:1 | 48.06 |
| N$_{1.75}$ | 1.75:1 | 56.31 |
| N$_{2.00}$ | 2.00:1 | 62.25 |

larger the mole ratio of 1-naphthaldehyde to BPA, the higher the gel content.

### 3.3. Mechanical and thermal properties

Fig. 6(a) and (b) shows the dependence of storage modulus ($E'$s) and tan $\delta$ of NE$_{0.50}$, NE$_{0.67}$, NE$_{0.80}$ and DGEBA cured by DDS, respectively. All the naphthalene epoxies possessed higher $E'$s than DGEBA/DDS system in both glassy and
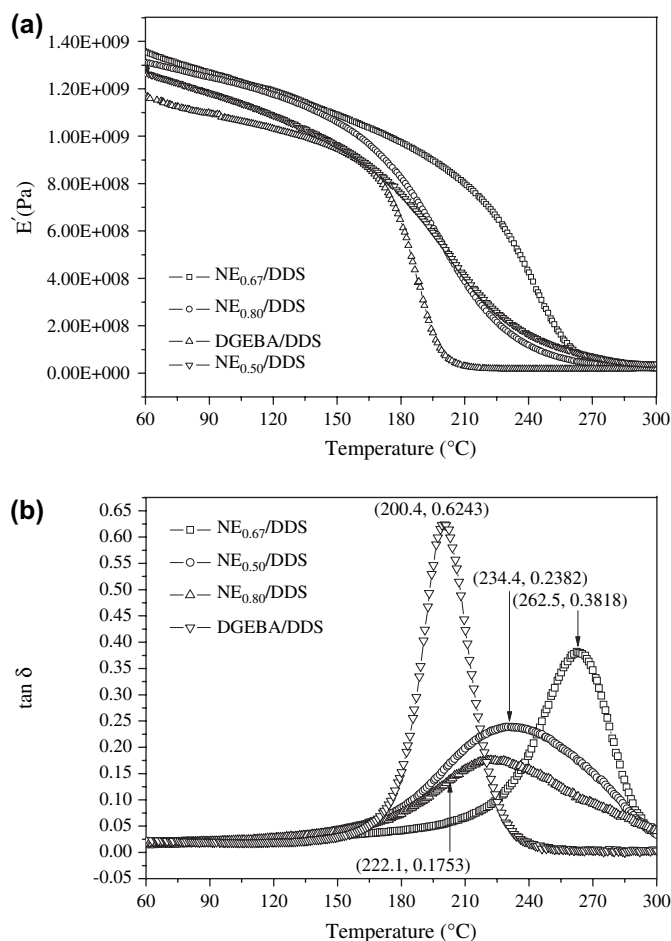


Fig. 6. Temperature dependences of storage modulus E′ and tan $\delta$ for cured NE$_{0.50}$/DDS, NE$_{0.67}$/DDS, NE$_{0.80}$/DDS and DGEBA/DDS.

rubbery regions. This was obviously the contribution of the rigid naphthalene moieties. However, the modulus was affected by the crosslinking density of epoxy resins. As shown in Table 5, one may find that the larger amount of naphthalene moieties resulted in lower degree of crosslinking. An increase of the crosslinking density can reduce the chain mobility and, consequently, increases the $T_g$ [19]. As a compromise, NE$_{0.67}$/DDS exhibited the highest $E'$.

The glass transition temperature was indicated by the peak of tan $\delta$. Again, one may notice that the naphthalene epoxy systems exhibited much higher $T_g$s than phenyl-based system. This can also be attributed to the high rigidity of naphthalene in the molecular backbone, which restrained the movements of the polymer segments. The NE$_{0.67}$/DDS system gave rise to the highest $T_g$ for the same reasons mentioned above.

Table 5
Average molecular weights and molecular polydispersity index of bis-NANER

| Sample | Ratio of 1-naphthaldehyde/BPA | $\overline{M}_n$ | $\overline{M}_w$ | PDI $(\overline{M}_w/\overline{M}_n)$ | EEW |
|---|---|---|---|---|---|
| NE$_{0.50}$ | 0.50:1 | 777 | 1373 | 1.77 | 227 |
| NE$_{0.67}$ | 0.67:1 | 963 | 2222 | 2.04 | 244 |
| NE$_{0.80}$ | 0.80:1 | 1356 | 3128 | 2.31 | 294 |
| NE$_{1.00}$ | 1.00:1 | 1531 | 4646 | 3.03 | 357 |

Thermal stability was assessed by thermogravimetric analysis (TGA) under nitrogen atmosphere, which are shown in Fig. 7 and Table 6. The temperature corresponding 10% weight loss, $T_{10}$, was taken as an index of thermal stability [20]. It can be seen that the thermal stability of naphthalene epoxy exhibited a maximum with $NE_{0.80}$/DDS system. Similar to above properties, the thermal stability was also controlled by two factors: naphthalene content and crosslinking density. When the content of naphthalene was lower, the system was not sufficiently thermal resistant; when the content of naphthalene was higher, the decreased crosslinking degree also causes a decrease in the thermal stability. DGEBA/DDS possessed the lowest char yield, and the char yield increased with the amount of naphthalene linearly.

### 3.4. Moisture absorption

In the practical usage, absorbed moisture was found to plasticize the epoxy resin [21], causing a lowering of the $T_g$ [22—26] and in turn affecting mechanical properties. The moisture absorption measurement is shown in Table 7. It showed that all cured naphthalene epoxy resins ($NE_{0.50}$, $NE_{0.67}$, $NE_{0.80}$ and $NE_{1.00}$) had better moisture resistance



Fig. 7. TGA traces of (a) $NE_{0.50}$/DDS; (b) $NE_{0.67}$/DDS; (c) $NE_{0.80}$/DDS; (d) $NE_{1.00}$/DDS and (e) DGEBA/DDS.

Table 6
Thermogravimetric analysis of cured polymers

| Sample code | $T_5$[a] (°C) | $T_{10}$[b] (°C) | $T_{max}$[c] (°C) | Char yield at 600 °C (%) | Char yield at 800 °C (%) |
|---|---|---|---|---|---|
| (a) | 355 | 365 | 410 | 25.12 | 20.72 |
| (b) | 376 | 386 | 412 | 27.39 | 25.27 |
| (c) | 375 | 387 | 413 | 30.88 | 27.10 |
| (d) | 356 | 369 | 411 | 33.87 | 28.92 |
| (e) | 366 | 376 | 419 | 17.66 | 17.66 |

[a] $T_5$, temperature of 5% weight loss.

[b] $T_{10}$, temperature of 10% weight loss.

[c] $T_{max}$, temperature of maximum rate of weight loss under nitrogen atmosphere.

Table 7
Moisture absorption of cured epoxy resins

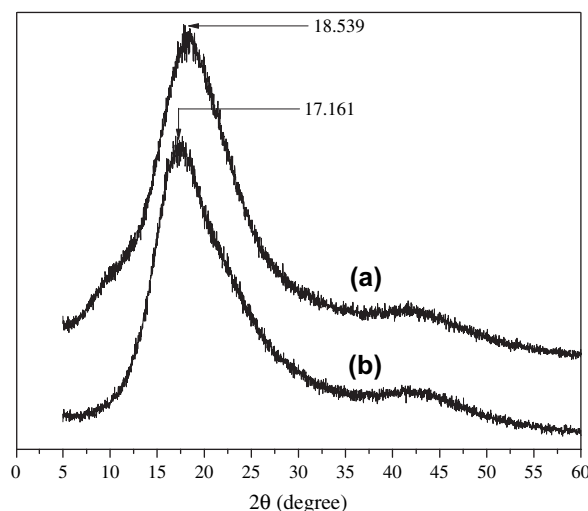| Sample code | Water absorption gains (wt%) | | | | |
|---|---|---|---|---|---|
| | 12 h | 24 h | 36 h | 48 h | 72 h |
| $NE_{0.50}$/DDS | 1.578 | 1.919 | 2.235 | 2.388 | 2.441 |
| $NE_{0.67}$/DDS | 1.474 | 2.045 | 2.123 | 2.268 | 2.308 |
| $NE_{0.80}$/DDS | 1.424 | 1.960 | 2.038 | 2.220 | 2.271 |
| $NE_{1.00}$/DDS | 1.358 | 2.012 | 2.083 | 2.163 | 2.211 |
| DGEBA/DDS | 1.418 | 1.639 | 1.964 | 2.397 | 2.501 |



Fig. 8. WAXD patterns for cured systems of (a) $NE_{0.67}$/DDS and (b) DGEBA/DDS.

than that of BPA epoxy system, and the hydrophobicity increased with increasing molar ratio of 1-naphthaldehyde to BPA. Obviously, the hydrophobic naphthalene moieties were responsible for the lower moisture absorption. Moreover, during the curing process, −OH groups were generated via ring opening of epoxy groups [27—30]. With the mole ratios of 1-naphthaldehyde to BPA increasing, the ring opening of epoxy reduced, thus less −OH groups were produced leading to a higher hydrophobicity of the system.

### 3.5. Wide-angle X-ray diffraction patterns

Fig. 8 shows the room temperature wide-angle X-ray diffraction diagrams of $NE_{0.67}$/DDS and DEGBA/DDS cured systems. The absence of noticeable diffractions primarily indicated that both systems were amorphous. However, the difference in the center of the two broad arches suggested that the packing was different in two polymers. Calculated from the location of the peaks, the average inter-segment distance in $NE_{0.67}$/DDS and DEGBA/DDS systems was 4.78 Å and 5.16 Å, respectively, which suggested that the former system was more densely compacted.

### 4. Conclusions

The novel epoxy resins containing naphthalene moiety were successfully synthesized via condensation of bisphenol A
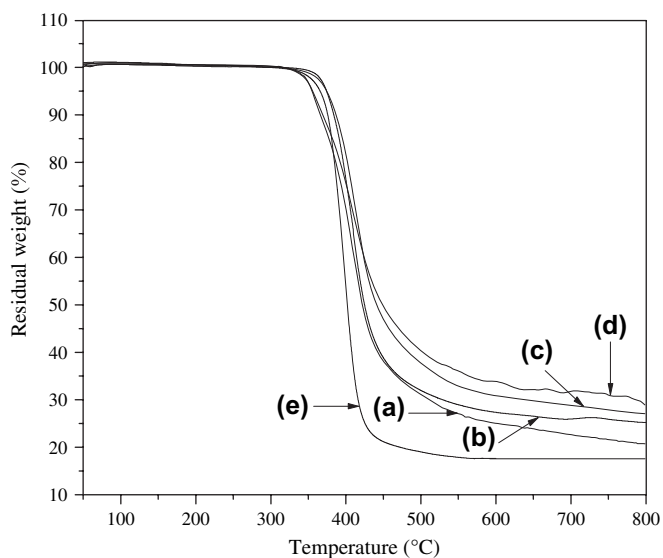
and 1-naphthaldehyde at various molar ratio, followed by epoxidation with epichlorohydrin. With the introduction of naphthyl in the skeleton, the resulting epoxy polymers cured with DDS exhibited higher glass transition temperatures, higher thermal stability and better moisture resistance than diglycidyl ether of bisphenol A (DGEBA). When the molar ratio of 1-naphthaldehyde to bisphenol A was 0.67, the optimal thermal resistance was observed. These pronounced good properties make it an attractive candidate for electronic encapsulation applications and composite materials.

## Acknowledgements

## References

[1] Bucknall CB, Gillbert AH. Polymer 1989;30(2):213–7.
[2] Wang CS, Lee MC. Polymer 2000;41(10):3631–8.
[3] Rwei SP, Cheng CY, Liou GS, Cheng KC. Polym Eng Sci 2005;45(4): 478–86.
[4] Wang CS, Lee MC. J Appl Polym Sci 1999;73(9):1611–22.
[5] Matsumoto A, Hasegawa K, Fukuda A. Polym Int 1993;30(1):65–72.
[6] Ohta K, Kosaka W, Yanagisawa K. Eur Patent 0,428,871 A2, 1991.
[7] Wang CS, Lee MC. J Appl Polym Sci 1998;70(10):1907–21.
[8] Yang CP, Chen WT. J Polym Sci Part A Polym Chem 1993;31(11): 2799–807.
[9] Xu K, Chen MC, Zhang K, Hu JW. Polymer 2004;45(4):1133–40.
[10] Kaji M, Endo T. J Polym Sci Part A Polym Chem 1999;37(16):3063–9.
[11] Ho TH. Macromol Mater Eng 2000;283(1):57–61.
[12] Duann YF, Liu TM, Cheng KC, Su WF. Polym Degrad Stab 2004; 8(2):305–10.
[13] Gouri C, Reghunadhan Nair CP, Ramaswamy R. Polym Int 2001;50(4): 403–13.
[14] Ho TH, Wang CS. J Appl Polym Sci 1999;74(8):1905–16.
[15] Lin CH, Chiang JC, Wang CH. J Appl Polym Sci 2003;88(11):2607–14.
[16] Liu YF, Zhang C, Du ZJ, Li HQ. J Appl Polym Sci 2006;99(3):858–68.
[17] Macko JA, Ishida H. J Polym Sci Part B Polym Phys 2000;38(20): 2687–701.
[18] Unnikrishnan KP, Thachil ET. Int J Polym Mater 2006;55(6):385–98.
[19] McKenna GB. In: Booth C, Price C, editors. Comprehensive polymer sciences polymer properties, vol. 2. Oxford: Pergamon Press; 1990. p. 311–5.
[20] Snow AW, Buckley LJ. Macromolecules 1997;30(3):394–405.
[21] Lee MC, Peppas NA. Prog Polym Sci 1993;18(5):947–61.
[22] McKague EL, Reynolds JD, Halkies JE. J Appl Polym Sci 1978; 22(6):1643–54.
[23] Mijovic J, Lin KF. J Appl Polym Sci 1985;30(6):2527–49.
[24] Musto P, Mascia L, Ragosta G, Scarinzi G, Villano P. Polymer 2000; 41(2):565–74.
[25] Xiao GZ, Shanahan MER. Polymer 1998;39(14):3253–60.
[26] Boinard E, Pethrick RA, Dazel-Job J, Macfarlane CJ. J Mater Sci 2000;35(8):1931–7.
[27] Sbirrazzuoli N, Mititelu-Mija A, Luc V, Alzina C. Thermochim Acta 2006;447(1):167–77.
[28] Catalani A, Bonicelli MG. Thermochim Acta 2005;438(1):126–30.
[29] Vyazovkin S, Sbirrazzuoli N. Macromolecules 1996;29(6):1867–73.
[30] Swier S, Assche GV, Vuchelen W, Bruno VM. Macromolecules 2005;38(6):2281–9.